Eur Radiol (2013) 23:3087–3093
DOI 10.1007/s00330-013-2910-2

MAGNETIC RESONANCE

Contrast-enhanced free-breathing 3D T1-weighted gradient-echo sequence for hepatobiliary MRI in patients with breath-holding difficulties

C. S. Reiner · A. M. Neville · H. K. Nazeer · S. Breault · B. M. Dale · E. M. Merkle · M. R. Bashir

Received: 15 February 2013 / Revised: 24 April 2013 / Accepted: 25 April 2013 / Published online: 4 June 2013

Abstract
Objective Evaluate the image quality and diagnostic performance of a free-breathing 3D-gradient-echo sequence with radial acquisition (rGRE) compared with a Cartesian breath-hold 3D-GRE (cGRE) sequence on hepatobiliary phase MRI in patients with breath-holding difficulties.
Methods Twenty-eight consecutive patients (15 males; mean age 61±11.9 years) were analysed in this retrospective IRB-approved study. Breath-holding difficulties during gadoxetate-disodium-enhanced liver MRI manifested as breathing artefacts during dynamic-phase imaging. MRI included axial and coronal cGRE and a radially sampled rGRE sequence during the hepatobiliary phase. Two radiologists independently evaluated cGRE and rGRE images for image quality, liver lesion detection and conspicuity, and bile duct conspicuity on a four-point scale.
Results Liver edge sharpness was significantly higher on rGRE images ($P<0.001$). Overall image quality was slightly but significantly higher for rGRE than for cGRE ($P<0.001$ and $P=0.039$). Bile duct conspicuity scores of rGRE and cGRE were not significantly different. Sensitivity for detection of the 26 liver lesions was similar for rGRE and cGRE (81-77 % and 73-77 %, $P=0.5$ and 1.0). Lesion conspicuity scores were significantly higher for rGRE for one reader ($P=0.012$).
Conclusion In patients with breath-holding difficulties, overall image quality and liver lesion conspicuity on hepatobiliary phase MRI can be improved using the rGRE sequence.

Key Points
- *Patients with diminished breath-holding capacities present a major challenge in abdominal MRI.*
- *A free-breathing sequence for hepatobiliary-phase MRI can improve image quality.*
- *Further advances are needed to reduce acquisition time of the free-breathing gradient-echo sequence.*

Keywords Image quality · Liver · Magnetic resonance imaging · T1-weighted free-breathing GRE sequence · Radial acquisition

C. S. Reiner · A. M. Neville · H. K. Nazeer · S. Breault · E. M. Merkle · M. R. Bashir (✉)
Department of Radiology, Duke University Medical Center, Duke North – Room 1417, Erwin Road, Durham, NC 27710, USA
e-mail: mustafa.bashir@duke.edu

B. M. Dale
Siemens Healthcare, Cary, NC, USA

E. M. Merkle
Department of Medical Radiology, University Hospital Basel, Basel, Switzerland

Introduction

Imaging patients with diminished breath-holding capacities presents a major challenge in abdominal magnetic resonance imaging (MRI). Patients in a substantial and increasing subset are unable to consistently suspend their respiration, including elderly patients, postoperative patients, and those with chronic medical conditions such as obesity and cardiopulmonary disease. Artefacts caused by motion degrade image quality and can even render images uninterpretable [1].

A clinical liver MRI protocol typically includes serial breath-holding sequences for dynamic contrast-enhanced imaging. Adequate image quality is essential for delineation of hepatic anatomical details and liver lesions. After serial breath-holds, patients with diminished respiratory capacity can fatigue, and their ability to breath-hold is further degraded. This can pose challenges particularly in liver MRI with hepatobiliary contrast agents, where the duration of the

examination and the number of breath-holds are typically greater than for studies performed with extracellular agents.

Efforts to mitigate respiratory artefacts have led to various strategies being proposed, including parallel imaging techniques to shorten the breath-hold time [2, 3], respiratory-triggered free-breathing techniques [4–6] and periodically rotated overlapping parallel lines with enhanced reconstruction technique (PROPELLER)-type sequences [7].

Recently, the use of radial data sampling for a three-dimensional (3D) T1-weighted gradient echo (GRE) sequence has been proposed as a free-breathing technique in abdominal MRI [8, 9]. This class of pulse sequence is similar to PROPELLER-type sequences in that the centre of k-space is visited multiple times during the acquisition, theoretically improving image contrast and motion robustness, but extending total imaging time [10]. More specifically, the radial technique evaluated in this study fills k-space using a "stack of stars" approach. One k-space line was acquired per repetition with standard 3D Cartesian phase encoding in the through-plane direction and radial encoding in the in-plane directions (i.e. each line passing through the centre of the k-space plane with a different angle for each line). One previous study found preliminary evidence that the free-breathing radial 3D GRE sequence may be useful for abdominal MRI in patients unable to suspend their respiration [9].

The purpose of our study was to evaluate the image quality and diagnostic performance of an isotropic free-breathing 3D T1-weighted GRE sequence with radial acquisition (rGRE) compared with standard axial and coronal breath-hold 3D T1-weighted Cartesian GRE (cGRE) sequences in hepatobiliary phase MRI in patients with breath-holding difficulties. Our hypothesis was that image quality, liver lesion detection and conspicuity, and potentially bile duct conspicuity would be improved by using the rGRE technique.

Materials and methods

Our institutional review board approved this Health Insurance Portability and Accountability Act-compliant retrospective study.

Study population

Between August and December 2011, 206 patients underwent MRI examinations of the liver with gadoxetate disodium (Gd-EOB-DTPA, Eovist/Primovist, Bayer HealthCare Pharmaceuticals Inc., Wayne, NJ, USA) including hepatobiliary phase imaging with a standard cGRE and a rGRE sequence at our institution. Of these patients, 28 with breath-holding difficulties were identified. A patient was deemed to have breath-holding difficulties if respiratory motion artefacts were present on any of the preceding dynamic phase acquisitions (portal venous or late dynamic phases). These 28 patients (15 men, 13 women; mean age: 61±11.9 years, range: 39–91 years) were included in the study. The subjects had a mean body weight of 84.6±24.0 kg (range: 54–145 kg), mean height of 174.8±5.6 cm (range: 163–188 cm), and mean body mass index of 28.0±6.4 kg/m^2 (range: 18.9–41.0 kg/m^2). Clinical indications for liver MRI included evaluation of focal liver lesions (n=6), diffuse liver disease (n=9), biliary pathological conditions (n=7), and oncological evaluation (n=6).

MR imaging

Magnetic resonance imaging was performed on a 1.5-T system (Magnetom Avanto, Siemens Healthcare) in the supine position using two anterior six-element body phased-array coils and three posterior three-element spine phased-array coils covering the upper abdomen. All subjects underwent a routine liver MRI protocol. For contrast-enhanced images, Gd-EOB-DTPA was injected at a standard dose of 10 ml, which corresponded to a mean adjusted dose of 0.04 mmol/kg bodyweight (range, 0.025–0.05 mmol/kg), with an injection rate of 2 ml/s with an automatic power injector, followed by a 20-ml saline chaser [11–13]. The MRI protocol included a 3D breath-hold (BH) axial fat-suppressed T1-weighted gradient echo (cGRE) volumetric interpolated breath-hold examination (VIBE) dynamic phase sequence with a slice thickness/gap of 4/0 mm, matrix size of 256×192, field of view (FOV) of 38–42 cm, voxel size of approximately 1.5×2.0×4 mm, and a parallel imaging factor of 2 for the portal venous (75 s post-contrast agent injection), and a late dynamic phase (~240 s post-contrast agent injection) [12, 13]. In the hepatobiliary phase (15–20 min post contrast injection) the cGRE sequence was performed in the axial and coronal planes with the following parameters: repetition time (TR), 4.3 ms; echo time (TE), 1.93 ms; flip angle, 30°; slice thickness/gap, 4/0 mm; matrix size, 256×192×60; field of view (FOV), 38–42 cm×75 %; voxel size approximately 1.5×2.0×4 mm; parallel imaging factor, 2. The rGRE sequence was performed between the axial and coronal cGRE sequences in the hepatobiliary phase. The patients were asked to perform shallow breathing during the free-breathing rGRE sequence. Parameters of the fat-suppressed T1-weighted rGRE sequence included: TR, 4.3 ms; TE, 1.93 ms; flip angle, 30°; slice thickness, 1.5 mm; matrix size, 256×256×144; FOV 38–42 cm; voxel size approximately 1.5×1.5×1.5 mm; no parallel acceleration. A high flip angle of 30° is used routinely at our institution in hepatobiliary phase imaging, owing to the benefit of the improved lesion and bile duct conspicuity compared with a conventional flip angle of 9–12° [14, 15]. Mean acquisition time for cGRE was 24 s each and for rGRE 4:40 min:s. For the purposes of this study, only cGRE images (axial and coronal) and rGRE images acquired in the hepatobiliary phase were evaluated.

Image analysis

Image analysis was performed by two independent radiologists (abdominal imaging fellow and fellowship-trained abdominal imaging attending with 4 years' post-fellowship experience) on a dedicated workstation (Leonardo, Siemens Healthcare, Erlangen, Germany). The hepatobiliary phase cGRE sequence (axial and coronal images) and the rGRE sequence were reviewed independently in random order. Readers were blinded to subject identifiers. rGRE images were viewed using the 3D viewer of the workstation displaying the images in the axial and coronal planes. Similarly, axial and coronal images of the cGRE sequence were reviewed side by side using the 2D viewer. Before reader review of the image data sets, one other radiologist assembled image examples from MR examinations not part of the study population for each image quality parameter and score. The readers reviewed these image examples and were encouraged to use the reference images throughout image interpretation, to reduce subjectivity in scoring.

Image quality

Image sets were evaluated for sharpness (blurring of liver contour, vessels, and bile ducts), image noise, streak artefacts, and overall image quality. For each of these parameters, a score from 4 to 1 was assigned as follows: for sharpness, 4=sharp, 3=mild blurring, not affecting interpretation, 2=moderate blurring, affecting interpretation, and 1=severe blurring, non-diagnostic; for image noise, 4=no visible image noise, 3=mild graininess, not affecting interpretation, 2=moderate graininess, affecting interpretation, and 1=severe graininess, non-diagnostic; for streak artefacts, 4=no visible streak artefacts, 3=mild artefacts, not affecting interpretation, 2=moderate artefacts, affecting interpretation, and 1=severe artefacts, non-diagnostic; for overall image quality, 4=excellent, 3=good, 2=satisfactory, but interfering with interpretation, and 1=poor, non-diagnostic. Although not typically seen with traditional cGRE imaging, we included the assessment for streak artefacts because these have been observed and reported for radial-type MRI and could potentially interfere with interpretation of the rGRE images. For axial and coronal cGRE images readers were asked to assign one overall score for the two sequences.

Bile duct and liver lesion evaluation

Readers rated the conspicuity of four bile duct segments (common bile duct, CBD; right hepatic duct, RHD; left hepatic duct, LHD; intrahepatic ducts, IHD) on a four-point scale (4=excellent, 3=good, 2=fair, 1=poor). If contrast material was not seen in a bile duct segment, a score of 0 was assigned to that segment.

For focal liver lesions with a short axis ≥3 mm, the readers recorded the appropriate liver segment, image number, and lesion long-axis size for each of the evaluated image sets. Up to five liver lesions were recorded per subject. The conspicuity of each liver lesion was scored from 4 to 1 (4=clearly visible, sharply marginated; 3=definitely visible, but indistinct margin or less conspicuous than 4; 2=subtle lesion; 1=very subtle, barely visible). In patients with more than five liver lesions, the conspicuity of two predefined lesions was assessed, and these lesions were excluded from the analysis of lesion detection. Detection of liver lesions was compared with a reference standard defined by a radiologist not involved in the image analysis. The reference standard was defined by reviewing all pulse sequences in each examination, as well as previous or follow-up imaging studies, and all available clinical and histopathological data. In patients with more than five liver lesions, the radiologist highlighted two random liver lesions for conspicuity assessment.

Statistical analysis

Image quality scores as well as conspicuity scores for bile ducts of cGRE and rGRE images were compared using the paired-sample Wilcoxon signed rank test. Liver lesion conspicuity scores of cGRE and rGRE images were compared using the unpaired Mann–Whitney U test to account for differences in lesion detection between the two sequences.

For calculation of sensitivity and specificity for liver lesion detection, subjects with more than five liver lesions were excluded. Sensitivity and specificity of cGRE and rGRE images were compared using McNemar's test.

The interobserver agreement between the two readers' interpretations of image quality, bile duct conspicuity, and liver lesion conspicuity was determined by calculating Cohen's weighted κ values and 95 % confidence intervals. The κ values were tested for a significant difference from zero. A κ value of <0.00 indicated no agreement; 0.00–0.20, slight agreement; 0.21–0.40, fair agreement; 0.41–0.60, moderate agreement; 0.61–0.80, substantial agreement; 0.81–1.00, almost perfect agreement [16].

Statistical analysis was performed using commercially available software (IBM SPSS Statistics, release 19.0, SPSS Inc., Chicago, IL, USA). Statistical significance was inferred at a P value less than 0.05.

Results

Image quality

The results of the image quality assessment for standard cGRE and rGRE sequences are summarised in Table 1. The rGRE sequence received significantly higher scores for sharpness than the cGRE sequence for both readers (P<0.001, Fig. 1).

Table 1 Image quality

	Reader 1			Reader 2		
	cGRE	rGRE	*P*-value	cGRE	rGRE	*P*-value
Sharpness	2.8±0.5	3.7±0.5	<0.001	2.6±0.7	3.4±0.7	<0.001
Image noise	3.1±0.8	3.0±0.6	0.62	3.0±1.0	2.7±0.8	0.106
Streak artefacts	4.0±0.0	2.9±0.5	<0.001	4.0±0.0	2.5±0.5	<0.001
Overall image quality	2.8±0.7	3.4±0.7	<0.001	2.5±0.9	2.9±0.8	0.039

cGRE, Cartesian breath-hold 3D fat-suppressed T1-weighted gradient echo sequence; rGRE, radial free-breathing 3D fat-suppressed T1-weighted gradient echo sequence

Mean scores for image noise were similar for cGRE images and for rGRE images for both readers (P=0.62 and 0.106). Streak artefacts were seen only on rGRE images, but none of the image sets was rendered non-diagnostic because of streak artefacts (Figs. 1 and 2). Overall image quality was significantly higher for rGRE images compared with cGRE images for both readers (P<0.001 and P=0.039). All rGRE image sets were of diagnostic image quality overall (score 2 to 4), whereas an average of 2 of the 28 cGRE image sets per reader were rated as non-diagnostic overall image quality (score 1).

Interreader agreement for image quality assessment of cGRE images was fair to almost perfect (sharpness: κ, 0.33; image noise: κ, 0.49; streak artefacts: κ, 1.00; overall image quality: κ, 0.58) and that for rGRE was fair to moderate (sharpness: κ, 0.52; image noise: κ, 0.51; streak artefacts: κ, 0.27; overall image quality: κ, 0.28).

Bile duct conspicuity

Contrast material excretion was seen in 86 of the 112 bile duct segments. In these segments, bile duct conspicuity was similar on cGRE and rGRE images with mean scores of 2.7 ±1.1 and 2.8±1.1 for reader 1 and 2.9±1.1 and 2.9±1.2 for reader 2 (P=0.79 and 0.829, Table 2). Interobserver agreement for evaluation of bile duct conspicuity was fair for cGRE (κ, 0.32) and moderate for rGRE (κ, 0.58) images.

Liver lesion detection and conspicuity

A total of 36 focal liver lesions were identified with the reference standard in 18 of the 28 subjects (14 cysts, 8 liver metastases, 4 haemangiomas, 3 dysplastic nodules, 2 hepatocellular carcinoma, 2 fibrotic lesions, 2 uncertain lesions, 1 subcapsular haematoma). Mean size of liver lesions was 1.45±0.98 cm (range: 0.3–3.8 cm). Twenty-one of the 36 (58 %) liver lesions measured 1 cm or less in diameter. Ten of the 28 subjects had no liver lesions. Five subjects had more than five liver lesions and were excluded from the calculation of liver lesion detection.

Sensitivity and specificity for liver lesion detection on cGRE and rGRE images assessed in 23 patients with a total of 26 liver lesions are given in Table 3. cGRE and rGRE

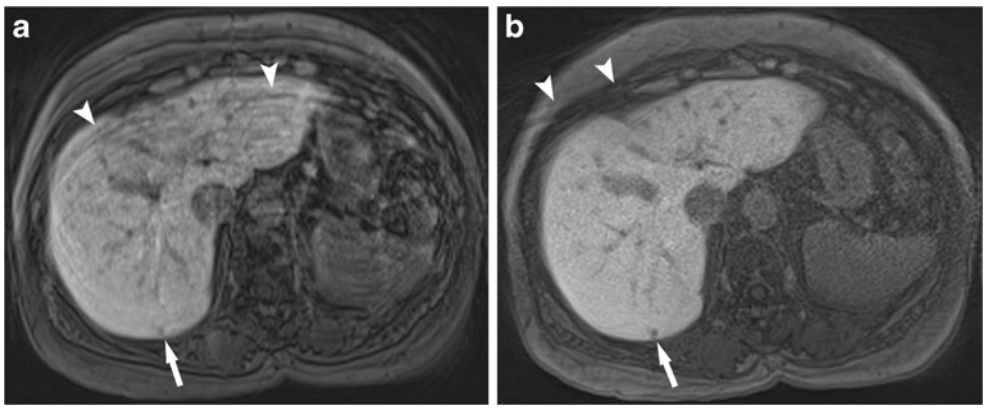

Fig. 1 A 59-year-old female patient imaged for evaluation of biliary dilation. **a** Axial Cartesian breath-hold 3D fat-suppressed T1-weighted gradient echo (cGRE) image in the hepatobiliary phase shows severe blurring of the liver owing to respiratory motion (*white arrowheads* in **a**). A small subcapsular cyst (6 mm) in liver segment VII is barely visible (*white arrow* in **a**) and was not detected by either reader. **b** Axial radial free-breathing 3D fat-suppressed T1-weighted gradient echo (rGRE) image in the hepatobiliary phase shows mild streak artefacts in the abdominal wall not affecting interpretation (*white arrowheads* in **b**). The liver lesion in segment VII is sharply delineated (*white arrow* in **b**) and was detected by both readers

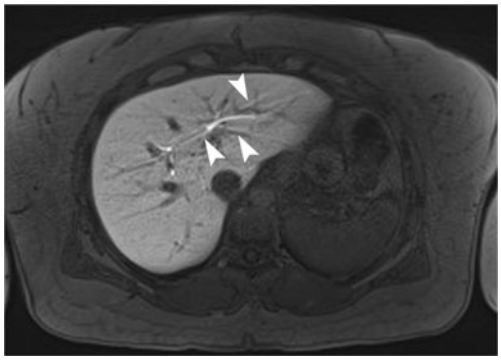

Fig. 2 A 64-year-old female patient imaged for evaluation of a liver lesion. Axial radial free-breathing 3D fat-suppressed T1-weighted gradient echo (rGRE) image shows streak-like artefacts around high-signal intrahepatic bile ducts (*white arrowheads*)

images showed similar sensitivities and specificities for liver lesion detection for both readers (P=0.5 and 1.0).

Liver lesion conspicuity of the 36 liver lesions was significantly higher when evaluating rGRE images compared with cGRE images for reader 1 (P=0.012, Table 2, Fig. 1). Interobserver agreement for evaluation of liver lesion conspicuity was fair for cGRE images (κ, 0.27) and moderate for rGRE images (κ, 0.47).

Discussion

The use of an rGRE sequence acquired during the hepatobiliary phase of liver MRI in subjects with breath-holding difficulties significantly improved image sharpness and overall image quality compared with a standard cGRE sequence in our study. Conspicuity of liver lesions was significantly higher on rGRE images in one of two readers, while sensitivity in liver lesion detection was similar. Bile duct conspicuity was comparable on rGRE and cGRE images in our study.

These results differ from those of two previous studies, where overall image quality was similar or lower for rGRE images acquired under free-breathing compared with cGRE images [8, 9]. A likely explanation is that those studies evaluated the use of this radial technique in patients in general, while we applied the technique to patients who had already demonstrated breath-holding difficulties in earlier parts of the MRI examination. In addition, in the study by Azevedo et al. [9], liver lesion conspicuity was significantly lower on unenhanced rGRE images compared with unenhanced cGRE images. The current study demonstrated improved lesion conspicuity using the radial technique, which may have been related in part to the intrinsically higher signal-to-noise ratio achieved with a contrast agent imaged in the hepatobiliary phase.

Previous efforts at reducing respiratory motion artefacts in patients with breath-holding difficulties have been successful [17, 18]. Altun et al. [17] used a magnetisation-prepared rapid gradient echo sequence, which is a motion-insensitive, single-slice acquisition technique for contrast-enhanced T1-weighted MRI of the abdomen in patients with breath-holding difficulties, and they found significantly better image quality compared with a standard BH 3D GRE sequence.

The concept of the radial acquisition of rectangular strips rotating through the centre of k-space was first proposed by Pipe [7] for motion-free brain and cardiac imaging. In abdominal imaging, the radial acquisition technique was first applied to T2-weighted sequences known as the PROPELLER (General Electric Medical Systems, Milwaukee, WI, USA) or BLADE (Siemens Medical Systems, Erlangen, Germany) techniques. Similar to the radial acquisition technique in our study, several recent studies have shown that this technique was able to substantially reduce in-plane respiratory motion artefacts and ghosting artefacts from bowel peristalsis and vascular pulsation [19, 20] and to improve liver lesion detection [21] on T2-weighted images of the liver.

A known disadvantage of the radial acquisition techniques is the occurrence of streak artefacts [8, 22]. Streak artefacts are caused by respiratory motion, but also result from undersampling in the periphery of k-space, which particularly occurs in larger patients. In addition, we anecdotally observed that the use of a small field of view, which results in positioning the arms outside the field of view, promotes the occurrence of streak artefacts [9]. In our study, image quality was partially degraded by streak artefacts on rGRE images, but none of the image sets was rendered non-diagnostic because of streak artefacts. Additionally, overall image quality improved despite the occasional presence of streak artefacts on the rGRE images, which were not observed on cGRE images.

We also noted streak-like artefacts on rGRE images from high-contrast structures such as the bile ducts and renal pelvises, which degraded image quality in some cases. In particular, a distortion of the contour of the bile ducts was sometimes observed (Fig. 2), although this did not diminish bile duct conspicuity compared to cGRE images.

Table 2 Bile duct and liver lesion conspicuity

	cGRE	rGRE	*P*-value
Bile duct conspicuity			
Reader 1	.2.7±1.1	2.8±1.1	0.79
Reader 2	2.9±1.1	2.9±1.2	0.829
Liver lesion conspicuity			
Reader 1	3.3±0.6	3.7±0.5	0.012
Reader 2	3.2±0.7	3.5±0.5	0.129

cGRE, Cartesian breath-hold 3D fat-suppressed T1-weighted gradient echo sequence; rGRE, radial free-breathing 3D fat-suppressed T1-weighted gradient echo sequence

Table 3 Sensitivity and specificity for liver lesion detection*

	cGRE		rGRE		*P*-value
	Sensitivity	Specificity	Sensitivity	Specificity	
Reader 1	76.9 % (20/26)	100.0 % (10/10)	80.8 % (12/26)	90.0 % (9/10)	0.5
Reader 2	73.1 % (19/26)	100.0 % (10/10)	76.9 % (20/26)	100.0 % (10/10)	1.0

*10 liver lesions in 5 subjects with >5 liver lesions were excluded for the calculation of lesion detection

cGRE, Cartesian breath-hold 3D fat-suppressed T1-weighted gradient echo sequence; rGRE, radial free-breathing 3D fat-suppressed T1-weighted gradient echo sequence

Image quality of rGRE images was reduced by image noise, which was attributed primarily to low slice thickness. Although we acquired the rGRE sequence with lower slice thickness than the cGRE sequence, image noise was not significantly different from cGRE images, consistent with the extended data acquisition time, and possibly as a benefit of oversampling the centre of k-space, an inherent advantage of radial techniques. None of the rGRE images was graded non-diagnostic because of severe image noise.

The advantage of acquiring isotropic, high-resolution images, for example, with a rGRE sequence, is that high quality multiplanar reformation is possible. We were able to generate coronal images from the axially acquired rGRE data set. It was not part of the study to compare axial and reformatted coronal rGRE images, but readers interpreted axial and reformatted coronal rGRE images together and assigned one score for each image quality parameter to axial and coronal images together. Furthermore, even 3D volume-rendering images with high liver-to-vessel contrast could be obtained from the isotropic rGRE data set in the hepatobiliary phase, which could be useful for liver segmentation or liver volumetry in surgical planning [23, 24].

Another approach for achieving a similarly high spatial resolution with the standard cGRE sequence would be to perform multiple averaging in a scan time similar to that of the rGRE sequence. Multiple averages allow for a certain reduction of motion; thus, cGRE could be used as a free-breathing sequence comparable to the rGRE sequence. However, a previous study comparing a free-breathing rGRE sequence and a free-breathing, multiple averaging cGRE sequence with identical spatial resolution found significantly lower image quality for the cGRE sequence [8].

Although the long acquisition time of the rGRE sequence is less problematic in the hepatobiliary phase than in dynamic phases, from a workflow perspective, it would be desirable to shorten the acquisition time. This technique could possibly be accelerated using parallel imaging schemes. Additionally, a multi-line blade acquisition approach rather than the line-by-line radial acquisition could reduce streak artefacts due to radial undersampling, and it has been employed successfully in T2-weighted radial techniques.

The results of previous studies suggest that there may be no benefit to the use of this technique in patients who can perform adequate breath-holding [8, 9]. A practical approach could be to screen dynamic BH images for respiratory motion artefacts, as proposed in our study, and add the rGRE sequence in the hepatobiliary phase in those cases where motion artefacts are observed or even to replace the standard cGRE sequences in the hepatobiliary phase with the rGRE sequence.

One limitation of our study was that the cGRE sequences and the rGRE sequence were acquired using different slice thicknesses, which leads to differences in image noise and sharpness. However, in the retrospective setting, we could not modify the image resolution for the purposes of the study. The rGRE sequence, similar to a navigated T1-weighted spoiled gradient echo sequence [25], is not limited to a single breath-hold and thus can take full advantage of the additional time available by acquiring isotropic voxels, which were considered useful for multiplanar reformatting. The original implementation of the rGRE sequence in our clinical protocol had been designed as an isotropic acquisition in order to provide improved visualisation of the biliary system, which is anatomically complex and may be more easily evaluated when free rotation of the imaging planes is possible. In addition, we assessed image quality by means of image appearance, such as sharpness, noise, and streak artefacts, rather than drawing direct conclusions regarding respiratory motion; this was because respiratory motion can have different appearances on images acquired radially or with a Cartesian k-space filling scheme. Motion can appear as general blurring or radial streaks; radial streaks can also be caused by in-plane respiratory motion or by undersampling. Thus, we chose to assess the appearances of the artefacts directly rather than attempting to draw specific conclusion regarding the sources of the artefacts.

A second limitation of our study is that we did not compare the rGRE sequence with a different high-resolution technique such as a navigated T1-weighted spoiled gradient echo sequence [25]. A more direct comparison would have been between the radial sampling and the Cartesian sampling with multiple averaging to arrive at the same resolution and scanning time.

However, multiple average GRE sequences were not available in our retrospective database. Additionally, we did not compare our study population with a control group without breath-holding difficulties to assess whether the improvement with rGRE is related to breath-holding difficulties or to other factors. However, the results of two previous studies have suggested no advantage for rGRE over cGRE in patients without breath-holding difficulties [8, 9].

In conclusion, in patients with breath-holding difficulties, overall image quality and liver lesion conspicuity on hepatobiliary phase MRI can be improved using the FB 3D GRE sequence. Further advances to reduce acquisition time and minimise streak artefacts are needed to further optimise the radial 3D FB GRE sequence.

Acknowledgements B.M.D. is an employee of Siemens Healthcare. E.M.M. receives research support from Siemens Healthcare and is a member of the speaker's bureau and a consultant for Bayer AG and consultant for Repligen. No conflicts of interest relevant to this work are reported.

M.R.B. receives research support from Siemens Healthcare and Bracco Diagnostics.

Conflicts of interest No conflicts of interest relevant to this work are reported.

References

1. Schultz CL, Alfidi RJ, Nelson AD, Kopiwoda SY, Clampitt ME (1984) The effect of motion on two-dimensional fourier transformation magnetic resonance images. Radiology 152:117–121
2. McKenzie CA, Lim D, Ransil BJ et al (2004) Shortening MR image acquisition time for volumetric interpolated breath-hold examination with a recently developed parallel imaging reconstruction technique: Clinical feasibility. Radiology 230:589–594
3. Vogt FM, Antoch G, Hunold P et al (2005) Parallel acquisition techniques for accelerated volumetric interpolated breath-hold examination magnetic resonance imaging of the upper abdomen: Assessment of image quality and lesion conspicuity. J Magn Reson Imaging 21:376–382
4. Klessen C, Asbach P, Kroencke TJ et al (2005) Magnetic resonance imaging of the upper abdomen using a free-breathing T2-weighted turbo spin echo sequence with navigator triggered prospective acquisition correction. J Magn Reson Imaging 21:576–582
5. Lee SS, Byun JH, Hong HS et al (2007) Image quality and focal lesion detection on T2-weighted MR imaging of the liver: Comparison of two high-resolution free-breathing imaging techniques with two breath-hold imaging techniques. J Magn Reson Imaging 26:323–330
6. Young PM, Brau AC, Iwadate Y et al (2010) Respiratory navigated free breathing 3D spoiled gradient-recalled echo sequence for contrast-enhanced examination of the liver: Diagnostic utility and comparison with free breathing and breath-hold conventional examinations. AJR Am J Roentgenol 195:687–691
7. Pipe JG (1999) Motion correction with PROPELLER MRI: Application to head motion and free-breathing cardiac imaging. Magn Reson Med 42:963–969
8. Chandarana H, Block TK, Rosenkrantz AB et al (2011) Free-breathing radial 3D fat-suppressed T1-weighted gradient echo sequence: A viable alternative for contrast-enhanced liver imaging in patients unable to suspend respiration. Invest Radiol 46:648–653
9. Azevedo RM, de Campos RO, Ramalho M, Heredia V, Dale BM, Semelka RC (2011) Free-breathing 3D T1-weighted gradient-echo sequence with radial data sampling in abdominal MRI: Preliminary observations. AJR Am J Roentgenol 197:650–657
10. Song HK, Dougherty L (2000) k-space weighted image contrast (KWIC) for contrast manipulation in projection reconstruction MRI. Magn Reson Med 44:825–832
11. Cruite I, Schroeder M, Merkle EM, Sirlin CB (2010) Gadoxetate disodium-enhanced MRI of the liver: Part 2, protocol pptimization and lesion appearance in the cirrhotic liver. AJR Am J Roentgenol 195:29–41
12. Feuerlein S, Boll DT, Gupta RT, Ringe KI, Marin D, Merkle EM (2011) Gadoxetate disodium-enhanced hepatic MRI: Dose-dependent contrast dynamics of hepatic parenchyma and portal vein. AJR Am J Roentgenol 196:W18–24
13. Ringe KI, Husarik DB, Sirlin CB, Merkle EM (2010) Gadoxetate disodium-enhanced MRI of the liver: Part 1, protocol optimization and lesion appearance in the noncirrhotic liver. AJR Am J Roentgenol 195:13–28
14. Bashir MR, Husarik DB, Ziemlewicz TJ, Gupta RT, Boll DT, Merkle EM (2012) Liver MRI in the hepatocyte phase with gadolinium-EOB-DTPA: Does increasing the flip angle improve conspicuity and detection rate of hypointense lesions? J Magn Reson Imaging 35:611–616
15. Frydrychowicz A, Nagle SK, D'Souza SL, Vigen KK, Reeder SB (2011) Optimized high-resolution contrast-enhanced hepatobiliary imaging at 3 tesla: A cross-over comparison of gadobenate dimeglumine and gadoxetic acid. J Magn Reson Imaging 34:585–594
16. Landis JR, Koch GG (1977) The measurement of observer agreement for categorical data. Biometrics 33:159–174
17. Altun E, Semelka RC, Dale BM, Elias J Jr (2008) Water excitation MPRAGE: An alternative sequence for postcontrast imaging of the abdomen in noncooperative patients at 1.5 Tesla and 3.0 Tesla MRI. J Magn Reson Imaging 27:1146–1154
18. Kim JH, Hong SS, Eun HW, Han JK, Choi BI (2012) Clinical usefulness of free-breathing navigator-triggered 3D MRCP in non-cooperative patients: Comparison with conventional breath-hold 2D MRCP. Eur J Radiol 81:e513–518
19. Hirokawa Y, Isoda H, Maetani YS, Arizono S, Shimada K, Togashi K (2008) MRI artifact reduction and quality improvement in the upper abdomen with PROPELLER and prospective acquisition correction (PACE) technique. AJR Am J Roentgenol 191:1154–1158
20. Rosenkrantz AB, Mannelli L, Mossa D, Babb JS (2011) Breath-hold T2-weighted MRI of the liver at 3T using the BLADE technique: Impact upon image quality and lesion detection. Clin Radiol 66:426–433
21. Hirokawa Y, Isoda H, Maetani YS et al (2009) Hepatic lesions: Improved image quality and detection with the periodically rotated overlapping parallel lines with enhanced reconstruction technique—evaluation of SPIO-enhanced T2-weighted MR images. Radiology 251:388–397
22. Hirokawa Y, Isoda H, Maetani YS, Arizono S, Shimada K, Togashi K (2008) Evaluation of motion correction effect and image quality with the periodically rotated overlapping parallel lines with enhanced reconstruction (PROPELLER) (BLADE) and parallel imaging acquisition technique in the upper abdomen. J Magn Reson Imaging 28:957–962
23. Catalano OA, Singh AH, Uppot RN, Hahn PF, Ferrone CR, Sahani DV (2008) Vascular and biliary variants in the liver: Implications for liver surgery. Radiographics 28:359–378
24. Lamade W, Glombitza G, Fischer L et al (2000) The impact of 3-dimensional reconstructions on operation planning in liver surgery. Arch Surg 135:1256–1261
25. Nagle SK, Busse RF, Brau AC et al (2012) High resolution navigated three-dimensional T(1)-weighted hepatobiliary MRI using gadoxetic acid optimized for 1.5 Tesla. J Magn Reson Imaging 36:890–899